mice were fed low-K^+ diets, significant hypokalemia was maintained, supporting that KSP-$OSR1^{-/-}$ mice had renal K^+ wasting.

In conclusion, the analysis of global $OSR1^{+/-}$ and KSP-$OSR1^{-/-}$ mice sheds some light on the physiological role of OSR1 in BP regulation and renal Na^+ handling. $OSR1^{+/-}$ mice exhibit hypotension associated with the reduced p-SPAK and p-NKCC1 abundance in aortic tissue and decreased p-NKCC2 with an increase in both p-SPAK and p-NCC in the kidney, which is indicative of a salt-wasting phenotype. KSP-$OSR1^{-/-}$ mice show markedly decreased p-NKCC2 expression in the TAL with a blunted response to furosemide and enhanced p-NCC expression in the DCT, supporting the notion that NKCC2 is the main target of OSR1 and accounts for the BS-like phenotype. These results show that OSR1 plays a dual role in arterial tonicity and renal Na^+ reabsorption, primarily through NKCC1 and NKCC2, respectively. The development of OSR1 inhibitors suppressing vascular NKCC1 and renal NKCC2 may be a promising direction for antihypertensive therapy in the future.

Materials and Methods

Blood and Urine Analysis and BP Measurement. The phenotype of male mice was evaluated at the age of 12–14 wk. Mice were kept in metabolic cages for 24-h urine collection. Urine osmolarities under ambient conditions were determined using spot urine samples. Blood pressure, plasma and urine electrolytes, and hormone were obtained and measured as previously described (17, 33).

Na^+ and K^+ Balance Study. The mice were raised on a 12-h day/night cycle, fed a normal rodent chow diet, and given plain drinking water ad libitum. For the evaluation of renal Na^+ and K^+ handing, a low-Na^+ diet or low-K^+ diet was fed for 6 d (34).

HCTZ and Furosemide Challenge Studies. HCTZ (12.5 mg/kg) and furosemide (15 mg/kg) were administered i.p., respectively, to the mice (19). Urine samples in the 4 h after a single-dose treatment were collected for analysis.

IB and Immunofluorescence Stain. Semiquantitative IB and immunofluorescence (IF) microscopy was carried out as previously described (17, 33). In addition to our previously generated rabbit anti–p-NCC (T53, T58, and S71) (17, 35), an antibody that could recognize both p-OSR1(S325) and p-SPAK(S383) simultaneously (14, 18), and rabbit anti–p-NKCC2 (T96), which could also recognize p-NKCC1(T206) (19), other commercially available primary antibodies used included rabbit anti-SPAK (Cell Signaling) (14, 18, 36), NKCC2 (Alpha Diagnostic) (19), NCC (Millipore) (17), mouse anti-OSR1 (Abnova) (14, 18), and NKCC (T4) (37). Alkaline phosphatase-conjugated anti-IgG antibodies (Promega) were used as secondary antibodies for IB, and Alexa 488 or 546 dye-labeled (Molecular Probes) secondary antibodies were used for IF microscopy. IF images were obtained using a LSM510 confocal microscope (Carl Zeiss).

Statistical Analysis. All results are expressed as mean ± SD. Results obtained for the $OSR1^{+/-}$ or KSP-$OSR1^{-/-}$ mice were compared with those from their WT littermates by means of the Student *t* test or, if the data violated a normal distribution, the nonparametric Mann–Whitney test. A *P* value less than 0.05 was considered to be statistically significant.

ACKNOWLEDGMENTS. We thank the Transgenic Mouse Model Core Facility of the National Research Program for Genomic Medicine, (NRPGM) and the National Core Facility Program for Biotechnology (NCFPB), National Science Council, Taiwan, for the provision of technical services. We also thank Yin Sun and Tai-Hsiang Chang for mice genotyping and preparation of tissue samples for IB and IF staining. This study was supported, in part, by the National Science Council, Taiwan (Grants NSC 100-2314-B-016-018-MY3 and NSC-98-2314-B-016-002-MY3), the Research Fund of Tri-Service General Hospital (Grant TSGH-C-100-040), and Japan-Taiwan Joint Research Program, Interchange Association, Japan.

1. Meyer JW, et al. (2002) Decreased blood pressure and vascular smooth muscle tone in mice lacking basolateral Na(+)-K(+)-2Cl(-) cotransporter. *Am J Physiol Heart Circ Physiol* 283:H1846–H1855.
2. Garg P, et al. (2007) Effect of the Na-K-2Cl cotransporter NKCC1 on systemic blood pressure and smooth muscle tone. *Am J Physiol Heart Circ Physiol* 292:H2100–H2105.
3. Wall SM, et al. (2006) Hypotension in NKCC1 null mice: Role of the kidneys. *Am J Physiol Renal Physiol* 290:F409–F416.
4. Kim SM, et al. (2008) Salt sensitivity of blood pressure in NKCC1-deficient mice. *Am J Physiol Renal Physiol* 295:F1230–F1238.
5. Gamba G (2005) Molecular physiology and pathophysiology of electroneutral cation-chloride cotransporters. *Physiol Rev* 85:423–493.
6. Orlov SN, Adragna NC, Adarichev VA, Hamet P (1999) Genetic and biochemical determinants of abnormal monovalent ion transport in primary hypertension. *Am J Physiol* 276:C511–C536.
7. Orlov SN, Tremblay J, Hamet P (2010) NKCC1 and hypertension: A novel therapeutic target involved in the regulation of vascular tone and renal function. *Curr Opin Nephrol Hypertens* 19:163–168.
8. Wilson FH, et al. (2001) Human hypertension caused by mutations in WNK kinases. *Science* 293:1107–1112.
9. Simon DB, et al. (1996) Bartter's syndrome, hypokalaemic alkalosis with hypercalciuria, is caused by mutations in the Na-K-2Cl cotransporter NKCC2. *Nat Genet* 13:183–188.
10. Simon DB, et al. (1996) Gitelman's variant of Bartter's syndrome, inherited hypokalaemic alkalosis, is caused by mutations in the thiazide-sensitive Na-Cl cotransporter. *Nat Genet* 12:24–30.
11. Tamari M, Daigo Y, Nakamura Y (1999) Isolation and characterization of a novel serine threonine kinase gene on chromosome 3p2. 3. *J Hum Genet* 44:2–116–21120.
12. Johnston AM, et al. (2000) SPAK, a STE20/SPS1-related kinase that activates the p38 pathway. *Oncogene* 19:4290–4297.
13. Piechotta K, Lu J, Delpire E (2002) Cation chloride cotransporters interact with the stress-related kinases Ste20-related proline-alanine-rich kinase (SPAK) and oxidative stress response 1 (OSR1). *J Biol Chem* 277:50812–50819.
14. Moriguchi T, et al. (2005) WNK1 regulates phosphorylation of cation-chloride-coupled cotransporters via the STE20-related kinases, SPAK and OSR1. *J Biol Chem* 280: 42685–42693.
15. Vitari AC, Deak M, Morrice NA, Alessi DR (2005) The WNK1 and WNK4 protein kinases that are mutated in Gordon's hypertension syndrome phosphorylate and activate SPAK and OSR1 protein kinases. *Biochem J* 391:17–24.
16. Huang CL, Yang SS, Lin SH (2008) Mechanism of regulation of renal ion transport by WNK kinases. *Curr Opin Nephrol Hypertens* 17:519–525.
17. Yang SS, et al. (2007) Molecular pathogenesis of pseudohypoaldosteronism type II: Generation and analysis of a Wnk4(D561A/+) knockin mouse model. *Cell Metab* 5: 331–344.
18. Ohta A, et al. (2009) Targeted disruption of the Wnk4 gene decreases phosphorylation of Na-Cl cotransporter, increases Na excretion and lowers blood pressure. *Hum Mol Genet* 18:3978–3986.
19. Yang SS, et al. (2010) SPAK-knockout mice manifest Gitelman syndrome and impaired vasoconstriction. *J Am Soc Nephrol* 21:1868–1877.
20. Cheng CJ, Shiang JC, Hsu YJ, Yang SS, Lin SH (2007) Hypocalciuria in patients with Gitelman syndrome: Role of blood volume. *Am J Kidney Dis* 49:693–700.
21. Delpire E, Gagnon KB (2008) SPAK and OSR1: STE20 kinases involved in the regulation of ion homoeostasis and volume control in mammalian cells. *Biochem J* 409:321–331.
22. Rafiqi FH, et al. (2010) Role of the WNK-activated SPAK kinase in regulating blood pressure. *EMBO Mol Med* 2:63–75.
23. Orlov SN, Mongin AA (2007) Salt-sensing mechanisms in blood pressure regulation and hypertension. *Am J Physiol Heart Circ Physiol* 293:H2039–H2053.
24. Kaplan MR, Plotkin MD, Brown D, Hebert SC, Delpire E (1996) Expression of the mouse Na-K-2Cl cotransporter, mBSC2, in the terminal inner medullary collecting duct, the glomerular and extraglomerular mesangium, and the glomerular afferent arteriole. *J Clin Invest* 98:723–730.
25. Guyton AC (1989) Roles of the kidneys and fluid volumes in arterial pressure regulation and hypertension. *Chin J Physiol* 32:49–57.
26. Oppermann M, et al. (2006) Macula densa control of renin secretion and preglomerular resistance in mice with selective deletion of the B isoform of the Na,K,2Cl co-transporter. *J Am Soc Nephrol* 17:2143–2152.
27. Oppermann M, et al. (2007) Renal function in mice with targeted disruption of the A isoform of the Na-K-2Cl co-transporter. *J Am Soc Nephrol* 18:440–448.
28. Bartter FC, Pronove P, Gill JR, Jr., MacCardle RC (1962) Hyperplasia of the juxtaglomerular complex with hyperaldosteronism and hypokalemic alkalosis. A new syndrome. *Am J Med* 33:811–828.
29. Kurtz I (1998) Molecular pathogenesis of Bartter's and Gitelman's syndromes. *Kidney Int* 54:1396–1410.
30. Takahashi N, et al. (2000) Uncompensated polyuria in a mouse model of Bartter's syndrome. *Proc Natl Acad Sci USA* 97:5434–5439.
31. Subramanya AR, Liu J, Ellison DH, Wade JB, Welling PA (2009) WNK4 diverts the thiazide-sensitive NaCl cotransporter to the lysosome and stimulates AP-3 interaction. *J Biol Chem* 284:18471–18480.
32. Richardson C, et al. (2011) Regulation of the NKCC2 ion cotransporter by SPAK-OSR1-dependent and -independent pathways. *J Cell Sci* 124:789–800.
33. Yang SS, et al. (2010) Generation and analysis of the thiazide-sensitive Na+ -Cl- cotransporter (Ncc/Slc12a3) Ser707X knockin mouse as a model of Gitelman syndrome. *Hum Mutat* 31:1304–1315.
34. Liu Z, et al. (2011) Downregulation of NCC and NKCC2 cotransporters by kidney-specific WNK1 revealed by gene disruption and transgenic mouse models. *Hum Mol Genet* 20:855–866.
35. Chiga M, et al. (2008) Dietary salt regulates the phosphorylation of OSR1/SPAK kinases and the sodium chloride cotransporter through aldosterone. *Kidney Int* 74:1403–1409.
36. Wang Y, et al. (2009) From the Cover: Whole-genome association study identifies STK39 as a hypertension susceptibility gene. *Proc Natl Acad Sci USA* 106:226–231.
37. Lytle C, Xu JC, Biemesderfer D, Forbush B, 3rd (1995) Distribution and diversity of Na-K-Cl cotransport proteins: A study with monoclonal antibodies. *Am J Physiol* 269:C1496–C1505.

The FASEB Journal • Research Communication

Involvement of aquaporin-7 in the cutaneous primary immune response through modulation of antigen uptake and migration in dendritic cells

Mariko Hara-Chikuma,*,†,[1] Yoshinori Sugiyama,† Kenji Kabashima,* Eisei Sohara,‡ Shinichi Uchida,‡ Sei Sasaki,‡ Shintaro Inoue,† and Yoshiki Miyachi*

*Department of Dermatology, Graduate School of Medicine, Kyoto University, Kyoto, Japan; †Innovative Beauty Science Laboratory, Kanebo Cosmetics Inc., Odawara, Japan; and ‡Department of Nephrology, Tokyo Medical and Dental University, Tokyo, Japan

ABSTRACT **Dendritic cells (DCs) have the ability to present antigen and play a critical role in the induction of the acquired immune response. Skin DCs uptake antigen and subsequently migrate to regional draining lymph nodes (LNs), where they activate naive T cells. Here we show that the water/glycerol channel protein aquaporin 7 (AQP7) is expressed on epidermal and dermal DCs and involved in the initiation of primary immune responses. AQP7-deficient DCs showed a decreased cellular uptake of low-molecular-mass compounds (fluorescein isothiocyanate and Lucifer yellow) and high-molecular-mass substances (ovalbumin and dextran), suggesting that AQP7 is involved in antigen uptake. AQP7-deficient DCs also exhibited reduced chemokine-dependent cell migration in comparison to wild-type DCs. Consistent with these *in vitro* results, AQP7-deficient mice demonstrated a reduced accumulation of antigen-retaining DCs in the LNs after antigen application to the skin, which could be attributed to decreased antigen uptake and migration. Coincidentally, AQP7-deficient mice had impaired antigen-induced sensitization in a contact hypersensitivity model. These observations suggested that AQP7 in skin DCs is primarily involved in antigen uptake and in the subsequent migration of DCs and is responsible for antigen presentation and the promotion of downstream immune responses.—Hara-Chikuma, M., Sugiyama, Y., Kabashima, K., Sohara, E., Uchida, S., Sasaki, S., Inoue, S., Miyachi, Y. Involvement of aquaporin-7 in the cutaneous primary immune response through modulation of antigen uptake and migration in dendritic cells. *FASEB J.* 26, 211–218 (2012). www.fasebj.org**

Key Words: macropinocytosis · phagocytosis · chemotaxis

THE SKIN PROVIDES A PERMEABILITY barrier and a highly refined system of immune surveillance to protect the body against unwanted substances, such as infectious agents, pathogens, or antigens from the environment. The immune system of the skin relies on a rich network of antigen-presenting dendritic cells (DCs) that localize in the epidermis and the dermis. Currently, skin DCs are divided into 3 subsets: epidermal Langerhans cells (LCs) and Langerin$^+$ or Langerin$^-$ dermal DCs (dDCs) (1, 2). DCs residing in the skin capture foreign antigens or pathogens, then mature and migrate to draining lymph nodes (LNs), where they present antigen to naive T cells and initiate immune responses (3–5). Immature DCs can constitutively uptake antigens by several pathways, such as macropinocytosis of soluble antigens; phagocytosis of particles, including viruses and bacteria; and receptor-mediated endocytosis (6, 7). Although the relative contributions of LCs or dDCs in antigen capture and processing remain undefined (8, 9), both are presumed to have key roles in eliciting cutaneous immune responses.

Aquaporins (AQPs) are integral membrane channel proteins that form a barrel-like structure surrounding pores, allowing the transport of water and other small solutes. To date, 13 AQPs (named AQP0–12) have been identified in mammals, and these are classified into 3 major subtypes according to their transport capabilities: water-selective AQPs (AQPs 1, 2, 4, and 5); aquaglyceroporins that transport water and possibly other small solutes, such as glycerol (AQPs 3, 7, 9, and 10); and unorthodox AQPs (AQPs 6, 8, 11, and 12) (10–12). The selectivity of the AQPs results both from a steric mechanism because of the pore size and from specific amino acid substitutions that regulate the preference for a hydrophobic or hydrophilic substrate (13, 14). Numerous studies have revealed the potential roles of AQPs in several organs and their functions, for example, AQPs 1–3 in the urinary concentrating system (15), AQP1 in angiogenesis (16), AQP3 in tumorigenesis (17), and AQP4 in neuromyelitis optica and brain edema (18, 19).

With regard to expression of AQPs in DCs, some

[1] Correspondence: Center for Innovation in Immunoregulative Technology and Therapeutics, Graduate School of Medicine, Kyoto University, Yoshida Konoe-cho, Sakyo-ku, Kyoto 606-8501, Japan. E-mail: haramari@kuhp.kyoto-u.ac.jp

doi: 10.1096/fj.11-186627

This article includes supplemental data. Please visit *http://www.fasebj.org* to obtain this information.

0892-6638/12/0026-0211 © FASEB

AQPs have been identified in DCs, including AQP3, 5, 7, and 9 in human DCs generated from peripheral blood mononuclear cells (PBMCs) (20, 21) and AQP5 in mice bone marrow monocyte-derived DCs (BMDCs) (22). Moreover, our preliminary experiment found that AQP3 and 7 were expressed in mice skin DCs. The study using AQP inhibitors in human PBMC-derived DCs suggested that AQPs might play a role in the process of antigen uptake *via* fluid phase macropinocytosis (20). The experiment on AQP5-knockout mice showed the decrease in endocytotic ability in AQP5-deficient BMDCs (22). These previous studies suggested the involvement of AQPs in antigen uptake in monocyte-derived DCs; however, a functional characterization of specific AQPs in cutaneous DCs has not yet been elucidated.

This study focuses on the role of AQP7 in skin DCs because another study from our laboratory found that AQP3 expression had little effect on DC function (unpublished results). We tested the hypothesis that AQP7 is involved in macropinocytosis and/or phagocytosis, specifically antigen uptake, which is required for antigen-induced cutaneous immune responses. For these studies, we utilized AQP7-deficient mice (23) and isolated LCs and dDCs from mouse skin. We found that AQP7 is functionally expressed in mouse skin DCs and is involved in antigen uptake, cell migration, and the subsequent initiation of an immune reaction. Our data suggest that AQP7 may play an important role in allergy induction and immune surveillance in the skin and in other tissues in which DCs are localized.

MATERIALS AND METHODS

Mice

AQP7-knockout ($AQP7^{-/-}$) mice (C57BL/6 genetic background) were generated by targeted gene disruption (23). All animal experiments were approved by the Committee on Animal Research of Kyoto University.

Cutaneous cell preparation and cultures

Skin was incubated with dispase (5 U/ml; Life Technologies, Grand Island, NY, USA) for 1 h at 37°C to separate the dermis and epidermis. The epidermis was incubated in enzyme-free cell dissociation buffer (20 min, 37°C; Millipore, Bedford, MA, USA) to isolate single cells. The dermis was incubated in collagenase type II (500 U/ml; Worthington Biochemicals, Lakewood, NJ, USA) for 1 h at 37°C. All solutions were dissolved in complete RPMI (cRPMI) containing 10% heat-inactivated fetal calf serum (Invitrogen, Carlsbad, CA, USA), 50 μM 2-mercaptoethanol (Sigma, St. Louis, MO, USA), 2 mM L-glutamine, 25 mM HEPES, 100 μM nonessential amino acids, and 10 μM sodium pyruvate (Invitrogen).

Quantitative RT-PCR

$CD11c^+$ cells were isolated from epidermal or dermal cell suspensions using CD11c microbeads with the AutoMACS system (Miltenyi Biotech, Gladbach, Germany) per the manufacturer's protocol. Total RNA was extracted using TRIzol (Invitrogen). The cDNA was reverse transcribed from total RNA samples using the Prime Script RT reagent kit (Takara Bio, Otsu, Japan). Quantitative RT-PCR was performed using SYBR Green I (Takara Bio) and the Light Cycler real-time PCR apparatus (Roche, Mannheim, Germany).

Immunofluorescence

The isolated LCs were cultured on polylysine-coated coverslips and were fixed with 4% formalin in PBS. Cells were permeabilized with 0.1% saponin and stained with anti-AQP7 (AB15568; Millipore) and a FITC-conjugated anti-rabbit IgG secondary antibody (Invitrogen).

Flow cytometry analysis

To determine AQP7 expression, single-cell suspensions were stained with monoclonal antibodies (Abs) against CD11c, MHC class II, and EpCAM (eBioscience, San Diego, CA, USA) and were fixed in 4% formalin. Cells were permeabilized with 0.1% Triton X-100 and incubated with anti-AQP7 (Millipore) and a FITC-conjugated anti-rabbit IgG secondary antibody (Invitrogen). The samples were analyzed using a Fortessa flow cytometer (BD Biosciences, Franklin Lakes, NJ, USA). For the analysis of DCs, cell suspensions were stained with antibodies recognizing CD11c, MHC class II, EpCAM, CD80, CD86, CCR7, and CXCR4 (eBioscience). Information regarding antibodies is available in Supplemental Table S1.

Macropinocytosis and phagocytosis assay

Freshly isolated epidermal or dermal cell suspensions were incubated in cRPMI for 1 h, followed with a Lucifer yellow CH potassium salt (LY, 0.1 mg/ml; Sigma), fluorescein isothiocyanate (FITC; 0.1–1 mg/ml; Invitrogen), FITC-dextran (molecular mass ~4, 40, 250 kDa, 0.5 mg/ml; Sigma), or FITC-ovalbumin (FITC-OVA; 0.25 mg/ml; Invitrogen) in cRPMI for 45 min (37°C, 5% CO_2). The cells were washed 4 times with cold PBS containing 1% BSA, stained with anti-MHC class II, and analyzed on a flow cytometer.

Water and glycerol permeability of LCs

Water and glycerol permeability were measured using a SX20 stopped-flow spectrometer (Applied Photophysics, Surrey, UK). Isolated LCs in RPMI medium (1×10^6 cells/μl) were subjected to a 150 mM inwardly directed mannitol or glycerol gradient at 22°C. Water uptake was measured by the kinetics of the decrease in cell volume, as measured by the 90° scattered light intensity at a wavelength of 450 nm, over the time course (24, 25). Glycerol uptake was estimated by a single exponential fit on the second part of the curve, as described previously (26). Reciprocal exponential time constants (τ^{-1}) were calculated.

Chemotaxis assay

Epidermal or dermal cell suspensions (10^6 cell/100 μl) were deposited into the upper chamber of a polycarbonate transwell membrane filter (5 μm pore size; Corning Costar, Cambridge, MA, USA). The lower chamber contained CXCL12 (100 ng/ml) or CCL21 (100 ng/ml) in cRPMI medium. After incubation for 3 h at 37°C, the recovered cells were analyzed using flow cytometry.

Contact hypersensitivity

Mice were sensitized by application of 20 μl of 2,4-dinitrofluorobenzene (DNFB; 0.5%) solution on the abdomen. After 5 d, 20 μl of DNFB (0.3%) was applied to the left ear, and the vehicle (acetone/olive oil, 4:1) was applied to the right ear. Ear swelling was measured with a thickness gauge (Teclok, Nagano, Japan) at 24 h after challenge.

DNFB-dependent cell proliferation and cytokine production were examined with cells (5×10^5) isolated from the axillary and inguinal LNs at 5 d after sensitization. The LN cells were cultured in the absence or presence of trinitrochlorobenzene (TNCB; 50 μg/ml) for 3 d, pulsed with 0.5 μCi [^{3}H]-thymidine for 24 h, and subjected to liquid scintillation counting. IFN-γ release into the culture supernatant during the entire 3-d period was determined using an ELISA kit (eBioscience).

For the adoptive transfer, cell suspensions obtained from the LNs of DNFB-sensitized mice were injected subcutaneously (2×10^5 cells/20 μl PBS) into the ears of naive WT mice. The ears were immediately challenged by applying 20 μl of 0.3% DNFB or vehicle to either side of the ear. Ear thickness was measured after 24 h.

Antigen-induced cutaneous DC migration

Mice were painted with 200 μl FITC (10 mg/ml in acetone and dibutyl phthalate, 1:1; Invitrogen) or 100 μl FITC-OVA (2 mg/ml in 50% ethanol; Invitrogen), and the number of migrated cutaneous DCs in the draining LNs was analyzed by flow cytometry. Before application of FITC-OVA, the stratum corneum was removed by tape stripping (3 or 10 times) to disrupt the skin permeability barrier, and the transepidermal water loss (TEWL) value was monitored with a Tewameter Vapo Scan (Asahi Biomed, Tokyo, Japan) as an index of barrier function (Asahi Biomed, Tokyo, Japan).

Statistical analysis

Statistical analysis was performed using a 2-tailed Student's *t* test or ANOVA.

RESULTS

AQP7 expression in mouse cutaneous DCs

To characterize the expression of AQP7 in cutaneous DCs, we analyzed AQP7 expression levels in mouse DCs, including epidermal LCs and dermal DCs (dDCs). The epidermis and dermis were separated by dispase treatment and digested into single-cell suspensions by an enzyme-free cell dissociation buffer or collagenase treatment, respectively. CD11c$^+$ cells were selected by AutoMACS bead separation from freshly isolated, functionally immature cells, and we analyzed AQP7 mRNA levels by quantitative real-time RT-PCR. An AQP7 transcript was identified in both LCs and dDCs as well as in CD4$^+$ T cells (**Fig. 1*A***). We also found that AQP3 was expressed in LCs and dDCs, while we did not identify AQP5 and AQP9 expression in skin DCs, implying that skin DCs might have different expression patterns of AQPs from BMDCs (Supplemental Fig. S1).

Using a germline AQP7$^{-/-}$ mouse as a control (23), we verified the expression of AQP7 protein in MHC class II$^+$ CD11c$^+$ EpCAM$^+$ LC populations from the epidermal cell suspension by flow cytometry analysis (Fig. 1*B*). Immunofluorescence microscopy showed that AQP7 was mainly localized on the plasma membrane of CD11c$^+$ LCs (Fig. 1*C*).

To examine the function of AQP7 in the development of skin DCs, we analyzed the cell density and size of DCs isolated from the epidermis and dermis. We observed comparable cell numbers and cell size between wild-type (WT) and AQP7$^{-/-}$ mice, indicating that AQP7 deficiency does not affect the generation of LCs or dDCs (Fig. 1*D*).

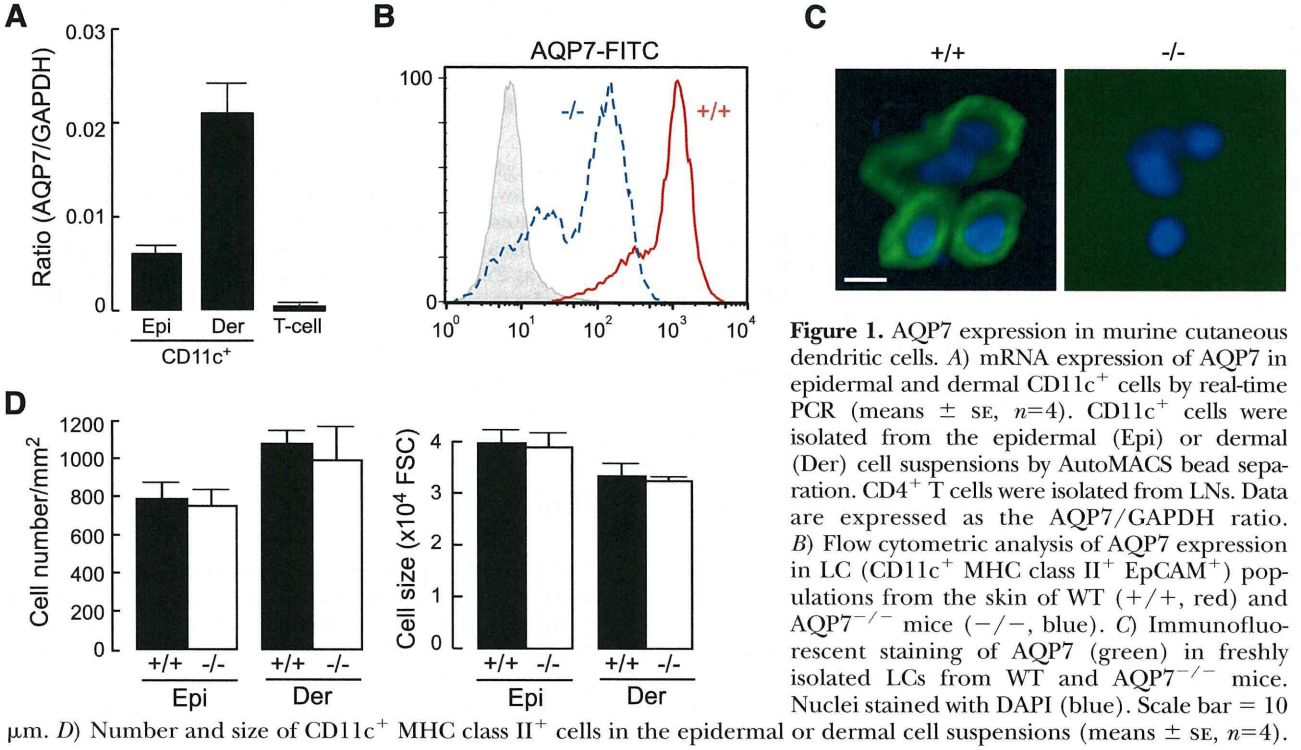

Figure 1. AQP7 expression in murine cutaneous dendritic cells. *A*) mRNA expression of AQP7 in epidermal and dermal CD11c$^+$ cells by real-time PCR (means ± SE, n=4). CD11c$^+$ cells were isolated from the epidermal (Epi) or dermal (Der) cell suspensions by AutoMACS bead separation. CD4$^+$ T cells were isolated from LNs. Data are expressed as the AQP7/GAPDH ratio. *B*) Flow cytometric analysis of AQP7 expression in LC (CD11c$^+$ MHC class II$^+$ EpCAM$^+$) populations from the skin of WT (+/+, red) and AQP7$^{-/-}$ mice (−/−, blue). *C*) Immunofluorescent staining of AQP7 (green) in freshly isolated LCs from WT and AQP7$^{-/-}$ mice. Nuclei stained with DAPI (blue). Scale bar = 10 μm. *D*) Number and size of CD11c$^+$ MHC class II$^+$ cells in the epidermal or dermal cell suspensions (means ± SE, n=4).

Impaired water/glycerol transport and antigen uptake in AQP7-deficient DCs

Previous studies using *Xenopus* oocytes expressing AQP7 found that AQP7 facilitates water and glycerol uptake (27, 28). We determined the osmotic water and glycerol permeability in isolated LCs from WT and AQP7$^{-/-}$ mice. The kinetics of the change in scattered light intensity in response to an osmotic challenge were measured as described previously (24, 25). Water transport in response to a 150 mM inwardly directed mannitol gradient was significantly higher in WT than in AQP7-deficient cells (**Fig. 2*A***). Glycerol permeability, measured by the stopped-flow technique, as described previously (26), was also decreased in the absence of AQP7 as compared to WT cells (Fig. 2*B*).

We next tested the hypothesis that AQP7 is involved in macropinocytosis and/or phagocytosis in DCs. First, we utilized FITC-labeled dextran, which is a commonly used model substance for pinocytosis and phagocytosis (6, 29). Epidermal or dermal cell suspensions were incubated with FITC-dextran, and the mean fluorescence intensity (MFI) of ingested FITC gated on MHC class II$^+$ cells was analyzed. Figure 2*C* shows that AQP7-deficient LCs had a reduced cellular uptake of FITC-dextran, which has components with molecular masses ranging from 4 to 250 kDa. In dDCs, AQP7 had an effect on the uptake of 4- to 40-kDa FITC-dextran molecules (Fig. 2*D*).

The FITC-dextran assay tests receptor-mediated endocytosis in the internalization of dextran because DCs express pattern recognition receptors that bind to carbohydrate moieties such as dextran (6, 29). We next utilized FITC and LY to more precisely examine macropinocytosis. Both FITC and LY uptake were significantly decreased in AQP7-deficient DCs compared to WT cells (Fig. 2*E, F*). These results indicate that AQP7 is involved in macropinocytosis in DCs.

Impaired chemotaxis in AQP7-deficient DCs

Immune responses are initiated when antigen-bearing DCs migrate from skin to LNs and activate T cells (3–5). Therefore, we examined the chemotaxis of skin DCs toward the ligands CXCL12 and CCL21 (30). Chemotaxis was significantly impaired in AQP7-deficient LCs and dDCs compared to WT cells (**Fig. 3*A***). The expression levels of the maturation markers CD80 and CD86 and of the chemokine receptors for migration, CCR7 and CXCR4, were comparable between WT and AQP7-deficient DCs (Fig. 3*B, C*). These findings suggested that AQP7 is involved not only in antigen uptake but also in the migration of DCs.

Because AQP7 was detected in CD4$^+$ T cells (Fig.

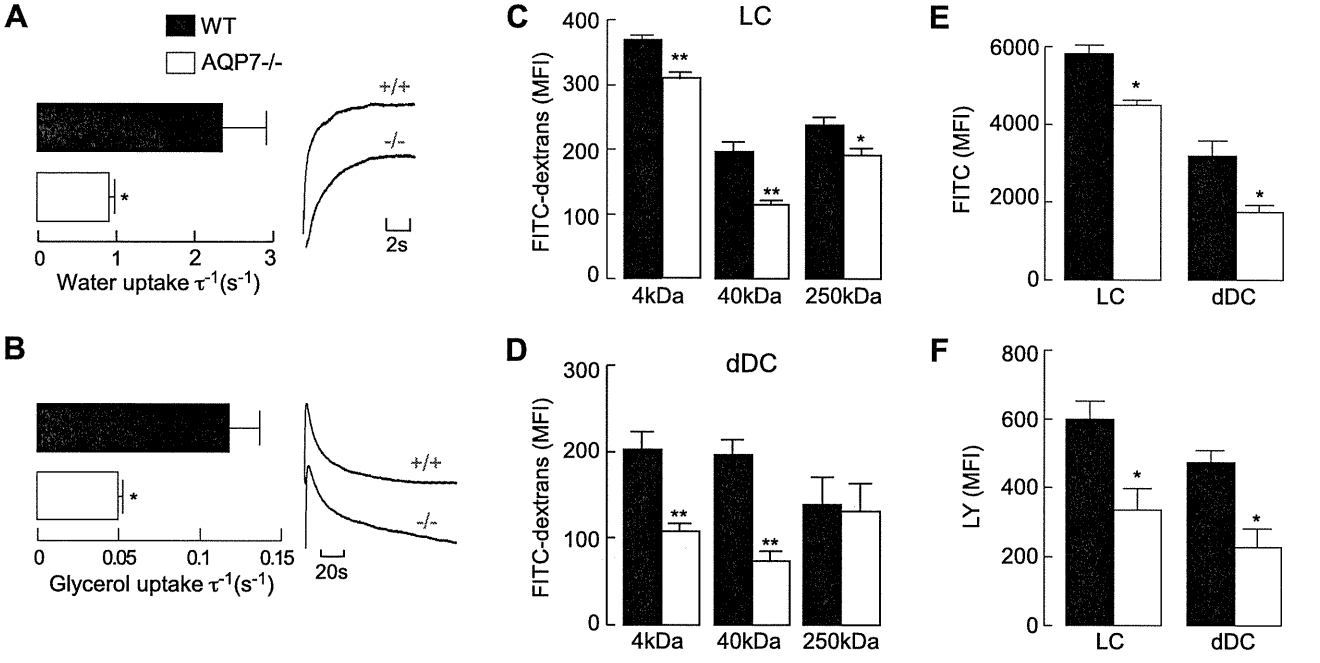

Figure 2. Impaired water/glycerol transport and macropinocytosis in AQP7-deficient DCs. *A*) Osmotic water permeability of LCs from WT and AQP7$^{-/-}$ mice was measured by scattered light intensity over the time course in response to a 150 mM inwardly directed mannitol gradient by stopped flow at 22°C. Reciprocal exponential time constant τ^{-1} was calculated (n=4). *$P < 0.01$. *B*) Glycerol permeability was measured in response to a 150 mM inward glycerol gradient by stopped flow at 22°C (n=4). *$P <$ 0.01. *C, D*) Cellular uptake of FITC-dextran. Epidermal (*C*) or dermal (*D*) cell suspensions were incubated with FITC-dextran (4, 40, or 250 kDa, 0.5 mg/ml) for 45 min at 37°C. Mean fluorescence intensity (MFI) of internalized FITC in MHC class II$^+$ cells was monitored (n=5). *$P < 0.05$, **$P < 0.01$. *E, F*) FITC (*E*) and LY (*F*) uptake by LCs and dDCs from WT and AQP7$^{-/-}$ mice. FITC or LY (0.1–1 mg/ml) was incubated in the cell suspension from the epidermis or dermis (45 min, 37°C). FITC or LY uptake was monitored by measuring the MFI of internalized FITC or LY in MHC class II$^+$ cells (n=4). *$P < 0.01$. Data are presented as means ± SE.

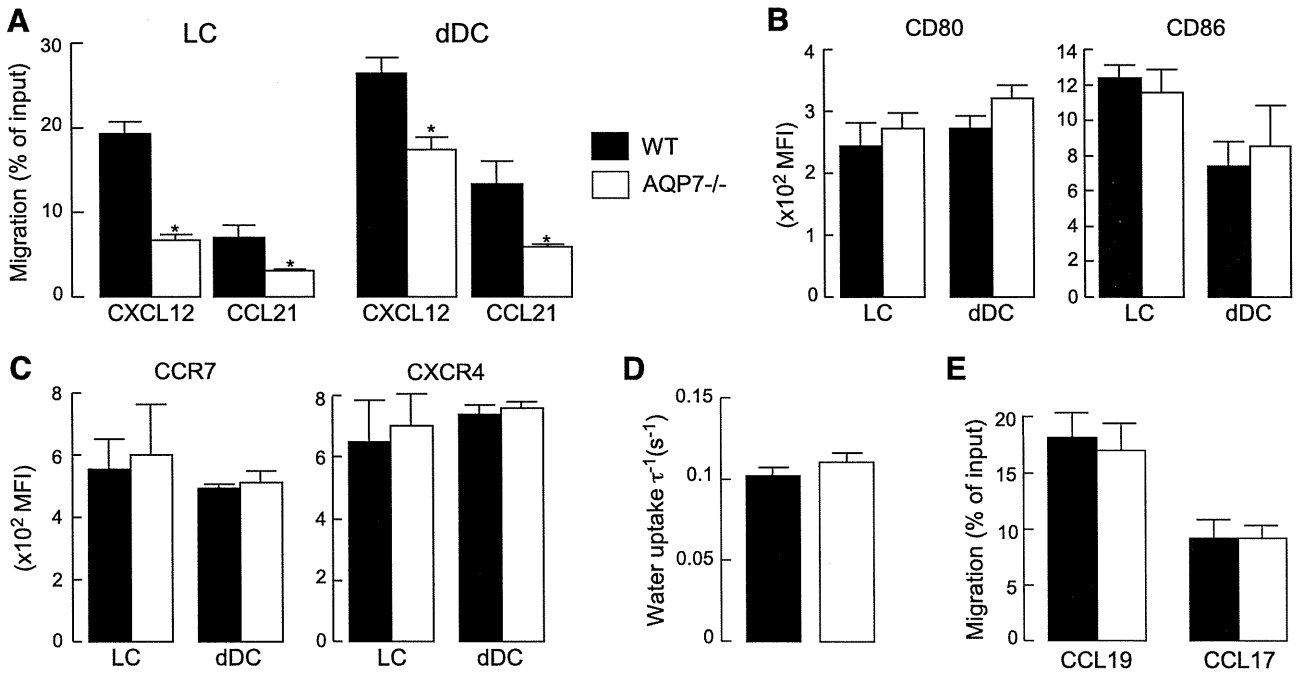

Figure 3. Impaired chemotaxis in AQP7-deficient DCs. *A*) Chemotaxis assay. Migration of DCs (epidermal or dermal cell suspensions) to the ligands CXCL12 (100 ng/ml) or CCL21 (100 ng/ml) was examined using a transwell chamber with 5-μm pores. Graphs show percentages of cells that migrated (n=5). *$P < 0.01$. *B, C*) Expression levels of maturation markers (*B*) and chemokine receptors involved in migration (*C*). Epidermal (for LCs) and dermal (for dDCs) cell suspensions were incubated in cRPMI for 2 d. MFI of CD80-APC$^+$, CD86-FITC$^+$, CCR7-PC7$^+$, and CXCR4-FITC$^+$ cells within the MHC class II$^+$ cell gate was determined (n=4). *D*) Osmotic water permeability in isolated CD4$^+$ T cells from WT and AQP7$^{-/-}$ mice (n=4). *E*) Chemotaxis assay of T cells. Migration of CD4$^+$ T cells to the ligands CCL19 (100 ng/ml) and CCL17 (100 ng/ml) was examined using a transwell chamber with 5-μm pores. Graphs show percentages of cells that migrated (n=5). Data are presented as means ± SE.

1*A*), we conducted a phenotypic analysis of T cells in the spleen, LNs, and thymus. CD4$^+$ and CD8$^+$ lymphocyte numbers (Supplemental Fig. S2) and the cell populations of CD3, CD25, CD44, and CD62L (not shown) in the LNs and thymus were similar between WT and AQP7-deficient mice. The water permeability of CD4$^+$ T cells (Fig. 3*D*) and chemotaxis toward CD4$^+$ T-cell ligands (Fig. 3*E*) were also comparable between WT and AQP7-deficient T cells, indicating that the expression of AQP7 likely has little effect on T-cell development or function.

Impaired OVA-induced sensitization in AQP7$^{-/-}$ mice

We next investigated the effect of AQP7-mediated antigen uptake and cell migration on antigen-induced sensitization. Here we utilized FITC-labeled OVA. OVA is the main protein in egg whites and is an established model allergen. Fluorescence microscopy showed the cellular uptake of FITC-OVA in LCs after a 1-h incubation (**Fig. 4*A***, left panel). Flow cytometry analysis demonstrated that AQP7-deficient LCs and dDCs had impaired incorporation of FITC-OVA (Fig. 4*A*, right panel).

We next sought to determine whether AQP7 has a role in antigen entry into the body, a process required for sensitization. To examine the effect of AQP7 deficiency on the response to the application of OVA on skin lesions, such as atopic dermatitis, the skin permeability barrier was disrupted by tape stripping (3 or 10 times) to remove the stratum corneum, and FITC-OVA was applied. The TEWL values of WT and AQP7$^{-/-}$ skin were comparable after tape stripping, indicating that barrier disruption occurred equally (Fig. 4*B*, left panel). The numbers of FITC$^+$ LCs and dDCs that migrated into the LNs were significantly impaired in AQP7$^{-/-}$ mice compared to WT mice (Fig. 4*B*, right panel). We next examined sensitization to OVA. We isolated a similar number of lymphocytes from the draining LNs of WT and AQP7$^{-/-}$ mice at 48 h after applying FITC-OVA, and the lymphocytes were incubated with OVA for 2 d. As shown in Fig. 4*C*, OVA-specific cell proliferation, as measured by [^{3}H]-thymidine incorporation, was impaired in AQP7-deficient cells compared to WT cells. These findings suggest that AQP7 is essential for antigen entry into the LNs following antigen-induced sensitization.

To investigate the involvement of AQP7 in antigen entry into the LNs using a different system, we utilized a FITC sensitization model wherein a FITC solution is applied to the skin, and cutaneous DCs take up FITC and migrate to the LNs for antigen presentation. Analysis of the skin-draining regional LNs at 24 h after FITC application showed a decrease in the accumulation of FITC$^+$ LCs and dDCs in AQP7$^{-/-}$ mice com-

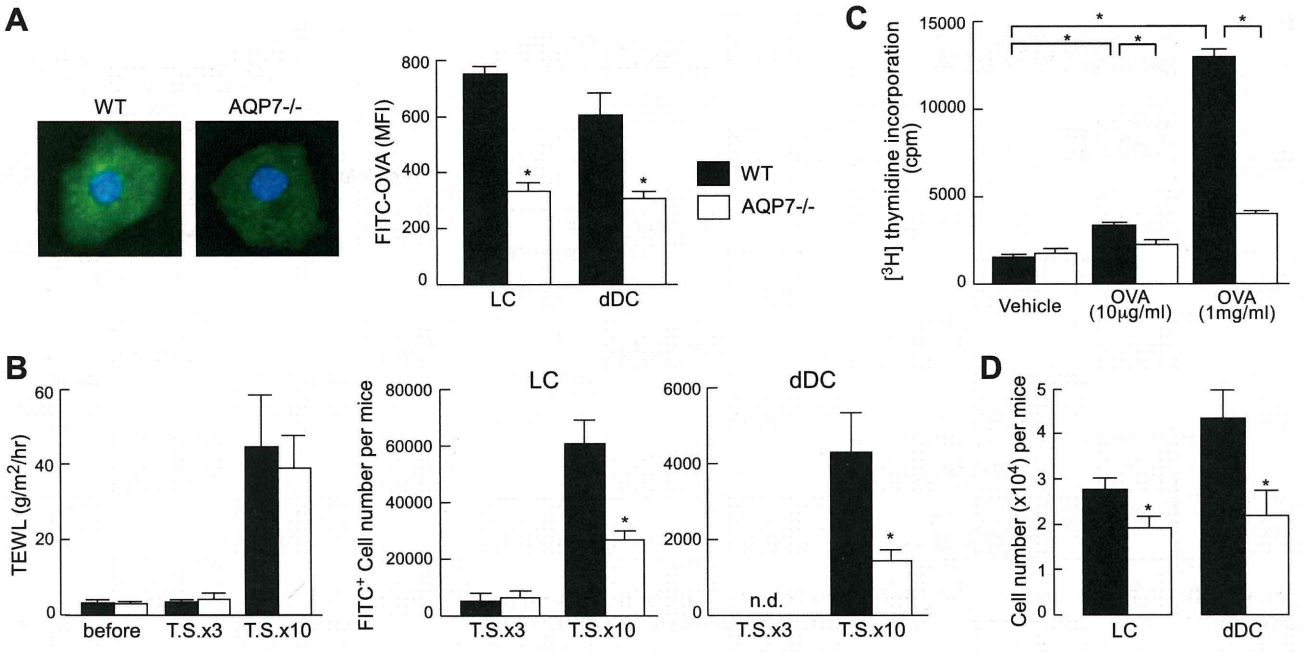

Figure 4. Impaired OVA-induced sensitization in AQP7$^{-/-}$ mice. *A*) Left panel: immunofluorescence microscopy of LCs incubated with FITC-OVA for 1 h at 37°C. Nuclei were stained with DAPI (blue). Right panel: cellular uptake of FITC-OVA. Epidermal or dermal cell suspensions were incubated with FITC-OVA (0.25 mg/ml) for 45 min at 37°C. MFI of internalized FITC was monitored (n=4). *B*) FITC-OVA migration *in vivo*. Skin permeability barrier was disrupted by tape stripping to remove the stratum corneum (3 or 10 times), and FITC-OVA was applied (100 μl of 2 mg/ml, 2×2 cm^2). Left panel: TEWL was measured as an index of barrier function after tape stripping. (Right panel: numbers of migrated LCs (CD11c$^+$ MHC class II$^+$ EpCAM$^+$) and dDCs (CD11c$^+$ MHC class II$^+$ EpCAM$^-$) 48 h after applying FITC-OVA (n=4). *C*) Antigen-specific cell proliferation was measured by [^{3}H]-thymidine incorporation. Lymphocytes (1×10^5 cells) isolated from the regional LNs of mice onto which FITC-OVA had been applied were incubated with vehicle or OVA (10 μg or 1 mg/ml) for 2 d (n=6). *D*) Skin DC migration into the draining LNs after FITC painting. WT and AQP7$^{-/-}$ mice were painted with 1% FITC solution (acetone and dibutylphthalate, 1:1) on the flank skin. At 24 h, LN cells were analyzed for the number of LCs (CD11c$^+$ MHC class II$^+$ EpCAM$^+$) or dDCs (CD11c$^+$ MHC class II$^+$ EpCAM$^-$) among FITC$^+$ cells by flow cytometry (n=5). Data are presented as means ± SE. *$P < 0.01$.

pared to WT mice (Fig. 4*D*). These data suggest the involvement of AQP7 in the induction of the primary immune response.

Impaired hapten-induced contact hypersensitivity and sensitization in AQP7$^{-/-}$ mice

To further determine the role of AQP7 in cutaneous immune reactions, we utilized a well-established hapten-induced contact hypersensitivity (CHS) model (31, 32). The WT and AQP7$^{-/-}$ mice were sensitized by applying DNFB to the abdomen, and the mice were challenged on the ear 5 d later. Ear swelling in response to the challenge, evidence of CHS, was significantly decreased in AQP7$^{-/-}$ mice compared to WT mice (**Fig. 5*A***). Histological examination confirmed that edema and the infiltration of lymphocytes into the dermis were attenuated in AQP7$^{-/-}$ mice, whereas these measures of inflammation were pronounced in WT skin (Fig. 5*A*, bottom panel).

To examine sensitization during the CHS response, antigen-specific cell proliferation and IFN-γ production were assayed. The lymphocytes from the draining LNs of WT and AQP7$^{-/-}$ mice were isolated at 5 d after DNFB sensitization, and the lymphocyte responses to TNCB, a water-soluble compound with the same antigenicity as DNFB, were compared *in vitro*. We observed a significant repression of antigen-induced cell proliferation and IFN-γ production in cells from AQP7$^{-/-}$ mice, indicating that T-cell activation during the sensitization period is impaired in the AQP7$^{-/-}$ mice.

Finally, we verified the impaired sensitization in AQP7$^{-/-}$ mice using subcutaneous adoptive transfer experiments. LN cells from sensitized WT and AQP7$^{-/-}$ mice were injected subcutaneously into the ears of naive recipient WT mice, which were challenged immediately with DNFB. As shown in Fig. 5*C*, the injected AQP7$^{-/-}$ cells suppressed ear swelling, and WT cells induced a strong CHS response. Collectively, these findings provide evidence that AQP7 expression is required for antigen-induced sensitization during the CHS response and that AQP7 might be responsible for antigen entry into the body.

DISCUSSION

Here we found that AQP7 is functionally expressed in skin DCs and is required for initiating cutaneous immune responses, such as CHS. An assay of macropinocytosis and/or phagocytosis showed that AQP7 defi-

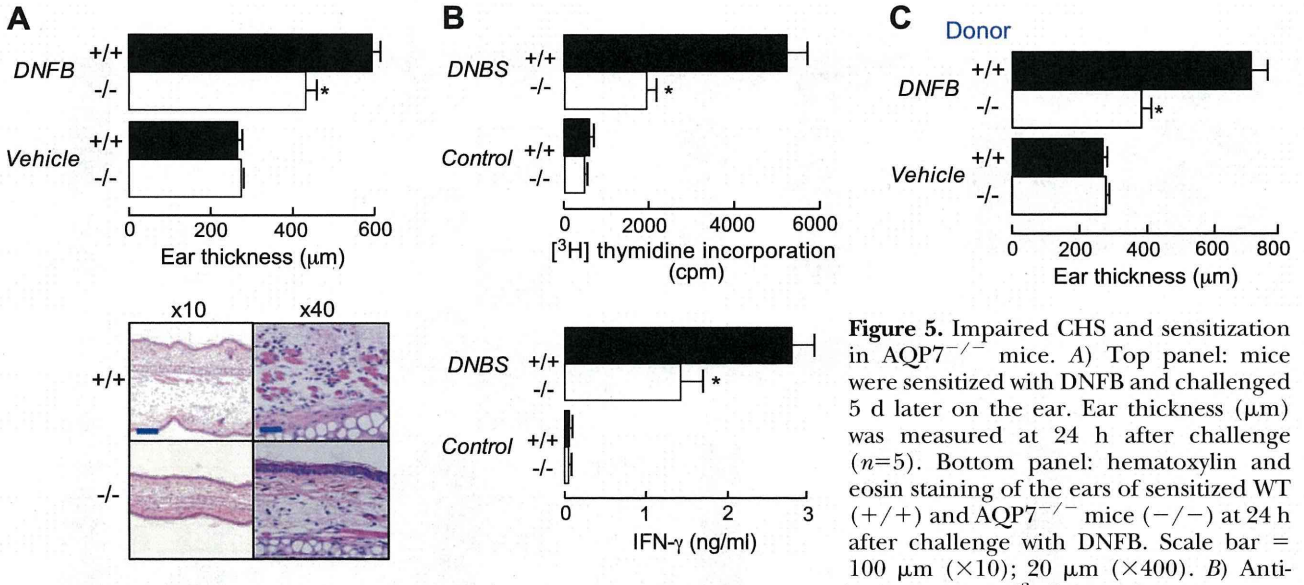

Figure 5. Impaired CHS and sensitization in AQP7$^{-/-}$ mice. *A*) Top panel: mice were sensitized with DNFB and challenged 5 d later on the ear. Ear thickness (μm) was measured at 24 h after challenge (n=5). Bottom panel: hematoxylin and eosin staining of the ears of sensitized WT (+/+) and AQP7$^{-/-}$ mice (−/−) at 24 h after challenge with DNFB. Scale bar = 100 μm (×10); 20 μm (×400). *B*) Antigen-specific cell proliferation (top panel) and IFN-γ production (bottom panel) during CHS. [^{3}H]-thymidine incorporation and IFN-γ production were determined in lymphocytes (1×10^5 cells) isolated from the regional LNs of DNFB-sensitized WT and AQP7$^{-/-}$ mice (n=5). *C*) Adoptive transfer experiments by subcutaneous injection. LN cells from sensitized donor WT and AQP7$^{-/-}$ mice (donor) were injected subcutaneously (2×10^5 cells) into the ear of naive recipient WT mice. Graph quantifies ear swelling at 24 h after challenge (n=4). Data are presented as means ± SE. *$P < 0.01$.

ciency decreased the cellular uptake of LY, FITC, FITC-OVA, and FITC-dextran into the skin DCs, including LCs and dDCs, suggesting the involvement of AQP7 in the capture of antigen. We also observed reduced cell migration toward ligands in AQP7-deficient DCs. In addition, AQP7$^{-/-}$ mice exhibited impaired antigen-induced sensitization after OVA or hapten application, and this impaired response was accompanied by suppressed lymphocyte proliferation. After application of a fluorescent antigen (FITC or FITC-OVA), the accumulation of antigen-retaining DCs in the LNs was decreased in AQP7$^{-/-}$ mice, which could be attributed to both the reduced captured of antigen and the reduced cell migration from skin to the LNs. Our findings provide the first evidence of the requirement for AQP7 in antigen-induced sensitization during an immune response.

DCs are antigen-presenting cells and are critical for the induction of primary immune responses. A previous study using human DCs derived from PBMCs showed that a mercury drug, one of the AQP inhibitors, blocked the macropinocytosis of LY but did not affect receptor-mediated endocytosis of FITC-dextran *via* the mannose receptor, suggesting that AQPs have a selective effect on macropinocytosis (20). In the study presented here, we demonstrated that AQP7 is involved in the cellular uptake of LY (MW 521), FITC (MW 389), FITC-conjugated dextran (MW ranging from 4 to 40 kDa), and FITC-OVA (MW ~45 kDa) into both LCs and dDCs, although it remains to be determined whether macropinocytosis, phagocytosis, or endocytosis was responsible for the uptake of these molecules. DCs express pattern-recognition receptors and bind to glycoproteins and other carbohydrate regions that are commonly expressed by pathogens (6, 33). Although the internalization of a soluble carbohydrate such as dextran into DCs occurs largely through receptor-mediated internalization, the assay using LY or FITC is thought to accurately examine macropinocytosis (6, 29). Therefore, our findings demonstrate that AQP7 is involved at least in macropinocytosis by skin DCs. After the intake of extracellular fluids by macropinocytosis, macrosolutes are concentrated and accumulate in a lysosomal compartment, which might depend on the selective transport of ions and water. We also demonstrated that AQP7 is required for water transport in DCs. AQP7-mediated water efflux might be responsible for regulating cell volume during macropinocytosis. Although further experiments are necessary to investigate the mechanism of AQP7-mediated antigen uptake, our data support the involvement of AQP7 in macropinocytosis.

In our studies, AQP7 was required for the chemotaxis of DCs, which might be important for antigen presentation and the subsequent initiation of the immune response. Previous studies have shown the involvement of some AQPs (AQP1, 3, and 4) in cell migration, for example, in angiogenesis or wound healing, in several endothelial and epithelial cell types (34, 35). The researchers of these studies proposed that AQP-mediated water transport was connected to actin dynamics during cell migration, although the cellular and molecular mechanisms that underlie this process are unclear. Again, macropinocytosis was found to be an actin-dependent process that requires the Rho-family GTPases, including Rac1 and Cdc42, for actin cytoskeletal rearrangements (33, 36). AQP7 might regulate the dynamics of actin reorganization, which regulates cell migration and macropinocytosis, and future studies will define the mechanism of AQP7-mediated DC migration.

In summary, our data provide the first evidence that AQP7 is required for the induction of primary cutane-

ous immune responses. Our findings suggest that AQP7 is primarily involved in antigen uptake and subsequently in the migration of epidermal LCs and dDCs, which are responsible for antigen processing and presentation and promote immune responses. Because DCs are localized not only in the skin but in most tissues of the body, AQP7 might have a causal role in allergy or unwanted immune reactions. Our findings suggest that blocking AQP7 by the use of topical drugs might be useful for the suppression of undesirable immune responses. FJ

The authors thank Maiko Yusa and Kiiko Kumagai for mouse breeding, Dr. Yoshinori Fujiyoshi and Akiko Kamegawa for help with water transport measurement, and Dr. Shunsuke Chikuma for critical reading of the manuscript. This work was supported in part by grants from the Ministry of Education, Culture, Sports, Science, and Technology of Japan.

REFERENCES

1. Merad, M., Ginhoux, F., and Collin, M. (2008) Origin, homeostasis and function of Langerhans cells and other langerin-expressing dendritic cells. *Nat. Rev. Immunol.* **8,** 935–947
2. Romani, N., Clausen, B. E., and Stoitzner, P. (2010) Langerhans cells and more: langerin-expressing dendritic cell subsets in the skin. *Immunol. Rev.* **234,** 120–141
3. Kripke, M. L., Munn, C. G., Jeevan, A., Tang, J. M., and Bucana, C. (1990) Evidence that cutaneous antigen-presenting cells migrate to regional lymph nodes during contact sensitization. *J. Immunol.* **145,** 2833–2838
4. Banchereau, J., Briere, F., Caux, C., Davoust, J., Lebecque, S., Liu, Y. J., Pulendran, B., and Palucka, K. (2000) Immunobiology of dendritic cells. *Annu. Rev. Immunol.* **18,** 767–811
5. Randolph, G. J., Angeli, V., and Swartz, M. A. (2005) Dendritic-cell trafficking to lymph nodes through lymphatic vessels. *Nat. Rev. Immunol.* **5,** 617–628
6. Norbury, C. C. (2006) Drinking a lot is good for dendritic cells. *Immunology* **117,** 443–451
7. Savina, A., and Amigorena, S. (2007) Phagocytosis and antigen presentation in dendritic cells. *Immunol. Rev.* **219,** 143–156
8. Noordegraaf, M., Flacher, V., Stoitzner, P., and Clausen, B. E. (2010) Functional redundancy of Langerhans cells and Langerin+ dermal dendritic cells in contact hypersensitivity. *J. Invest. Dermatol.* **130,** 2752–2759
9. Honda, T., Nakajima, S., Egawa, G., Ogasawara, K., Malissen, B., Miyachi, Y., and Kabashima, K. (2010) Compensatory role of Langerhans cells and langerin-positive dermal dendritic cells in the sensitization phase of murine contact hypersensitivity. *J. Allergy Clin. Immunol.* **125,** 1154–1156
10. Rojek, A., Praetorius, J., Frøkiaer, J., Nielsen, S., and Fenton, R. A. (2008) A current view of the mammalian aquaglyceroporins. *Annu. Rev. Physiol.* **70,** 301–327
11. Verkman, A. S. (2009) Aquaporins: translating bench research to human disease. *J. Exp. Biol.* **212,** 1707–1715
12. Carbrey, J. M., and Agre, P. (2009) Discovery of the aquaporins and development of the field. *Handb. Exp. Pharmacol.* **190,** 3–28
13. Savage, D. F., Egea, P. F., Robles-Colmenares, Y., O'Connell, JD, 3rd, and Stroud, R. M. (2003) Architecture and selectivity in aquaporins: 2.5 a X-ray structure of aquaporin Z. *PLoS Biol.* **1,** E72
14. Oliva, R., Calamita, G., Thornton, J. M., and Pellegrini-Calace, M. (2010) Electrostatics of aquaporin and aquaglyceroporin channels correlates with their transport selectivity. *Proc. Natl. Acad. Sci. U. S. A.* **107,** 4135–4140
15. Verkman, A. S. (2008) Dissecting the roles of aquaporins in renal pathophysiology using transgenic mice. *Semin. Nephrol.* **28,** 217–226
16. Saadoun, S., Papadopoulos, M. C., Hara-Chikuma, M., and Verkman, A. S. (2005) Impairment of angiogenesis and cell migration by targeted aquaporin-1 gene disruption. *Nature* **434,** 786–792
17. Hara-Chikuma, M., and Verkman, A. S. (2008) Prevention of skin tumorigenesis and impairment of epidermal cell proliferation by targeted aquaporin-3 gene disruption. *Mol. Cell. Biol.* **28,** 326–332
18. Lennon, V. A., Kryzer, T. J., Pittock, S. J., Verkman, A. S., and Hinson, S. R. (2005) IgG marker of optic-spinal multiple sclerosis binds to the aquaporin-4 water channel. *J. Exp. Med.* **202,** 473–477
19. Papadopoulos, M. C., and Verkman, A. S. (2007) Aquaporin-4 and brain edema. *Pediatr. Nephrol.* **22,** 778–784
20. De Baey, A., and Lanzavecchia, A. (2000) The role of aquaporins in dendritic cell macropinocytosis. *J. Exp. Med.* **191,** 743–748
21. Moon, C., Rousseau, R., Soria, J. C., Hoque, M. O., Lee, J., Jang, S. J., Trink, B., Sidransky, D., and Mao, L. (2004) Aquaporin expression in human lymphocytes and dendritic cells. *Am. J. Hematol.* **75,** 128–133
22. Wang, G. F., Dong, C. L., Tang, G. S., Shen, Q., and Bai, C. X. (2008) Membrane water permeability related to antigen-presenting function of dendritic cells. *Clin. Exp. Immunol.* **153,** 410–419
23. Sohara, E., Rai, T., Miyazaki, J., Verkman, A. S., Sasaki, S., and Uchida, S. (2005) Defective water and glycerol transport in the proximal tubules of AQP7 knockout mice. *Am. J. Physiol. Renal Physiol.* **289,** F1195–F2000
24. Yang, B., Kim, J. K., and Verkman, A. S. (2006) Comparative efficacy of HgCl2 with candidate aquaporin-1 inhibitors DMSO, gold, *TEA+*, and acetazolamide. *FEBS Lett.* **580,** 6679–6684
25. Tanimura, Y., Hiroaki, Y., and Fujiyoshi, Y. (2009) Acetazolamide reversibly inhibits water conduction by aquaporin-4. *J. Struct. Biol.* **166,** 16–21
26. Roudier, N., Verbavatz, J. M., Maurel, C., Ripoche, P., and Tacnet, F. (1998) Evidence for the presence of aquaporin-3 in human red blood cells. *J. Biol. Chem.* **273,** 8407–8412
27. Ishibashi, K., Kuwahara, M., Gu, Y., Kageyama, Y., Tohsaka, A., Suzuki, F., Marumo, F., and Sasaki, S. (1997) Cloning and functional expression of a new water channel abundantly expressed in the testis permeable to water, glycerol, and urea. *J. Biol. Chem.* **272,** 20782–20786
28. Kuriyama, H., Kawamoto, S., Ishida, N., Ohno, I., Mita, S., Matsuzawa, Y., Matsubara, K., and Okubo, K. (1997) Molecular cloning and expression of a novel human aquaporin from adipose tissue with glycerol permeability. *Biochem. Biophys. Res. Commun.* **241,** 53–58
29. Sallusto, F., Cella, M., Danieli, C., and Lanzavecchia, A. (1995) Dendritic cells use macropinocytosis and the mannose receptor to concentrate macromolecules in the major histocompatibility complex class II compartment: downregulation by cytokines and bacterial products. *J. Exp. Med.* **182,** 389–400
30. Dieu-Nosjean, M. C., Vicari, A., Lebecque, S., and Caux, C. (1999) Regulation of dendritic cell trafficking: a process that involves the participation of selective chemokines. *J. Leukoc. Biol.* **66,** 252–262
31. Grabbe, S., and Schwarz, T. (1998) Immunoregulatory mechanisms involved in elicitation of allergic contact hypersensitivity. *Immunol. Today* **19,** 37–44
32. Martin, S. F. (2004) T lymphocyte-mediated immune responses to chemical haptens and metal ions: implications for allergic and autoimmune disease. *Int. Arch. Allergy Immunol.* **134,** 186–198
33. Kerr, M. C., and Teasdale, R. D. (2009) Defining macropinocytosis. *Traffic* **10,** 364–371
34. Papadopoulos, M. C., Saadoun, S., and Verkman, A. S. (2008) Aquaporins and cell migration. *Pflügers Arch.* **456,** 693–700
35. Hara-Chikuma, M., and Verkman, A. S. (2008) Aquaporin-3 facilitates epidermal cell migration and proliferation during wound healing. *J. Mol. Med.* **86,** 221–231
36. West, M. A., Prescott, A. R., Eskelinen, E. L., Ridley, A. J., and Watts, C. (2000) Rac is required for constitutive macropinocytosis by dendritic cells but does not control its downregulation. *Curr. Biol.* **10,** 839–488

Received for publication April 19, 2011.
Accepted for publication September 15, 2011.